MADYN 2000 Version 4.5

The following new features and improvements were introduced in version 4.5:

1. Static Analyses with Fluid Film Bearings without Pre-Calculation
2. Automatic Analyses of Dynamic Fluid Film Bearing Characteristics
3. New Features for User Defined Fluids (seal analyses)
4. Improvement of Connections
5. Improvements of Fluid Film Bearing Analyses

Table of content for detailed description of features:

1. Static Analyses with Fluid Film Bearings without Pre-Calculation

Static analyses considering the shaft centreline position in fluid film bearings (i.e. the fluid film thickness) until version 4.4 required a precalculated table with the nonlinear relation between bearing force and journal in the form of a dimensionless table containing the journal position (dimensionless deflection ε, and angle γ) as a function of the dimensionless bearing load (Sommerfeld-number) and angle Φ_F. In case of statically overdetermined systems (rotors supported on more than 2 bearings) this analysis requires an iteration. The analysis starts with a rigid support (no compliance due to the fluid film), which yields a first estimate of the bearing force. The journal position in the bearing caused by the bearing force is then calculated yielding a new bearing force and a new position. The iteration stops if the change of force and position in an iteration step is sufficiently small. Until now the journal positions were interpolated from the precalculated table. The Sommerfeld numbers and the force angles had to cover the necessary range.

In version 4.5 the pre-calculation is no longer necessary. In each iteration step of the nonlinear static analysis the fluid film bearing program ALP3T is called returning the journal position, thus replacing the interpolation.

This considerably facilitates the static analysis in statically overdetermined systems in the presence of cross coupling forces. In such cases the resulting final position of the rotor is hard to predict. This applies for example for the following two rather common cases:

- Shaft trains with many bearings including fixed pad bearings causing a large component of the deflection perpendicular to the load.
- Shafts with many seals influencing the static deflection as it occurs in pumps. The seals contribute to the support of the pump due to the Lomakin effect, which makes a pump rotor always statically overdetermined even if it has only two bearings. Moreover, the seals have cross coupling forces.

Two such examples are shown in the following.

1.1 Example of a Shaft Train with many Bearings

An example of a shaft train with many bearings is shown in figure 1.1. The train also has a gear pinion with a mesh force. The bearings of the pinion are 2-lobe fixed pad bearings, all other bearings are 4-tillting pad bearings.

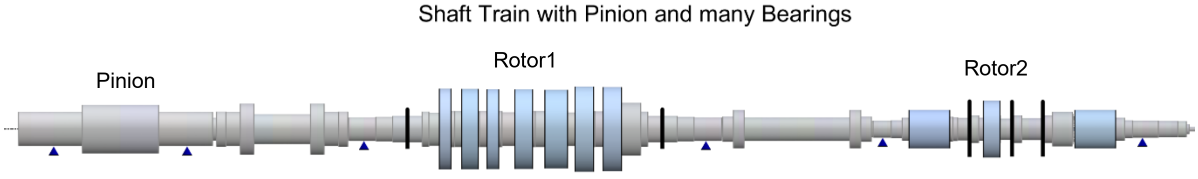

Fig. 1.1: Shaft train with a pinion and many bearings

Results of the static analysis with 100% gear load are shown in figure 1.2 (displacements) and figure 1.3 (forces). For comparison results of an analysis with rigid bearings are shown in figure 1.4 and 1.5. Displacements obviously are quite different and consequently the bearing forces, especially for the Rotor1 DE bearing.

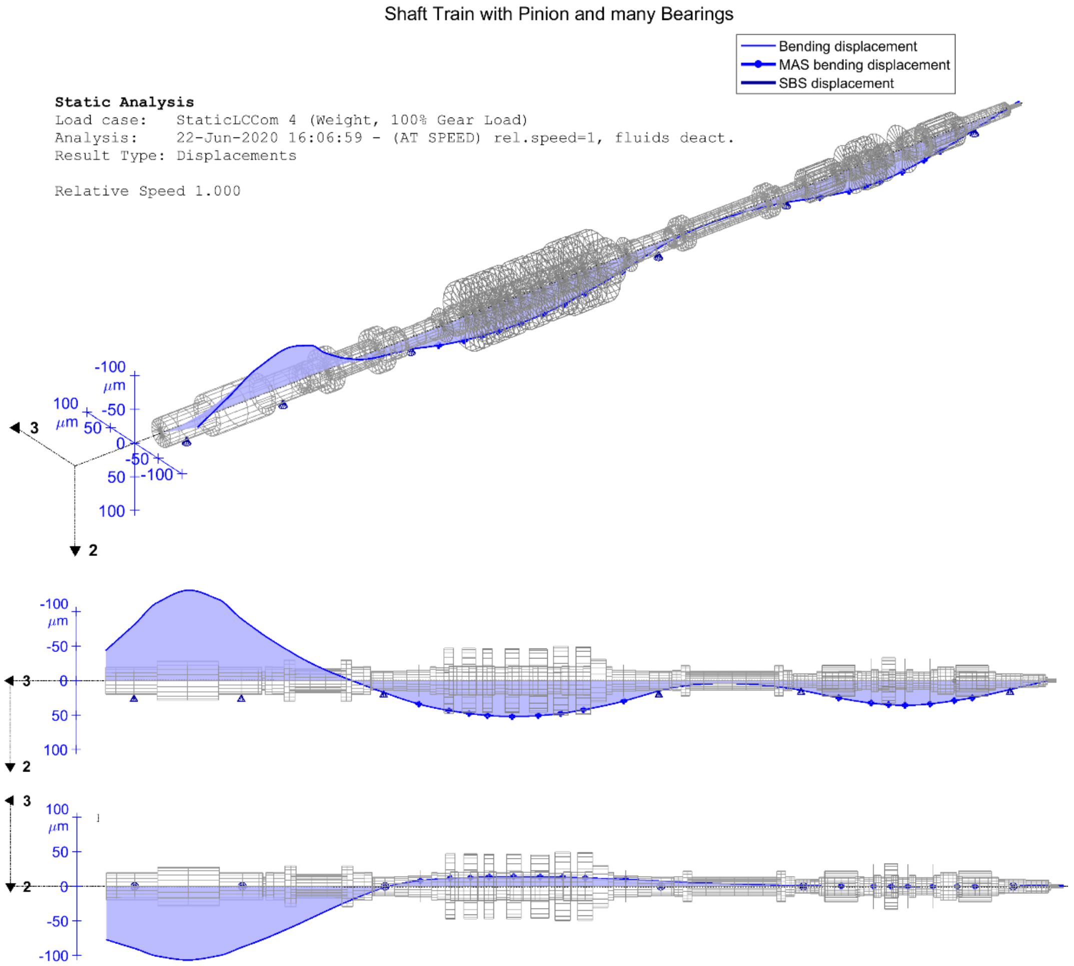

Fig. 1.2: Displacement of the shaft train with many bearings, results with oil film

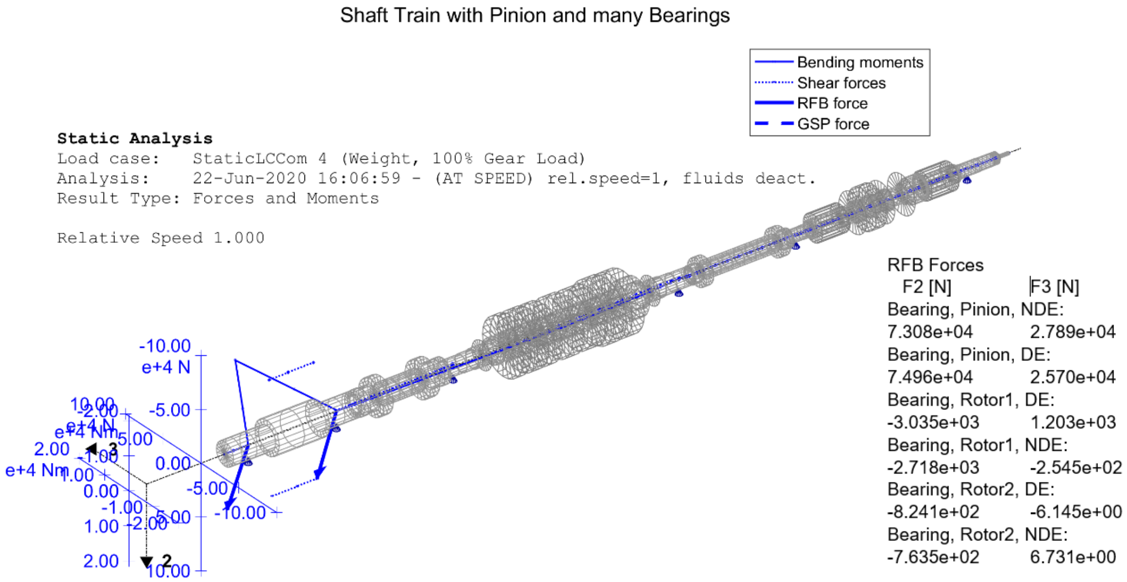

Fig. 1.3: Forces in the shaft train with many bearings, results with oil film

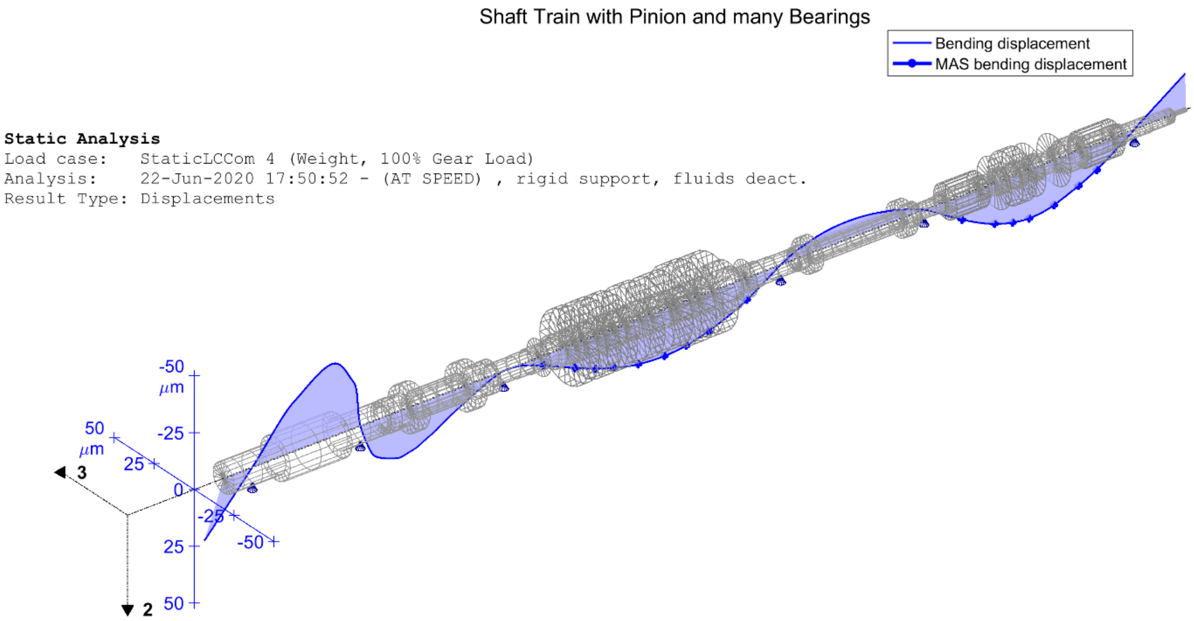

Fig. 1.4: Displacement of the shaft train with many bearings, results with rigid bearings

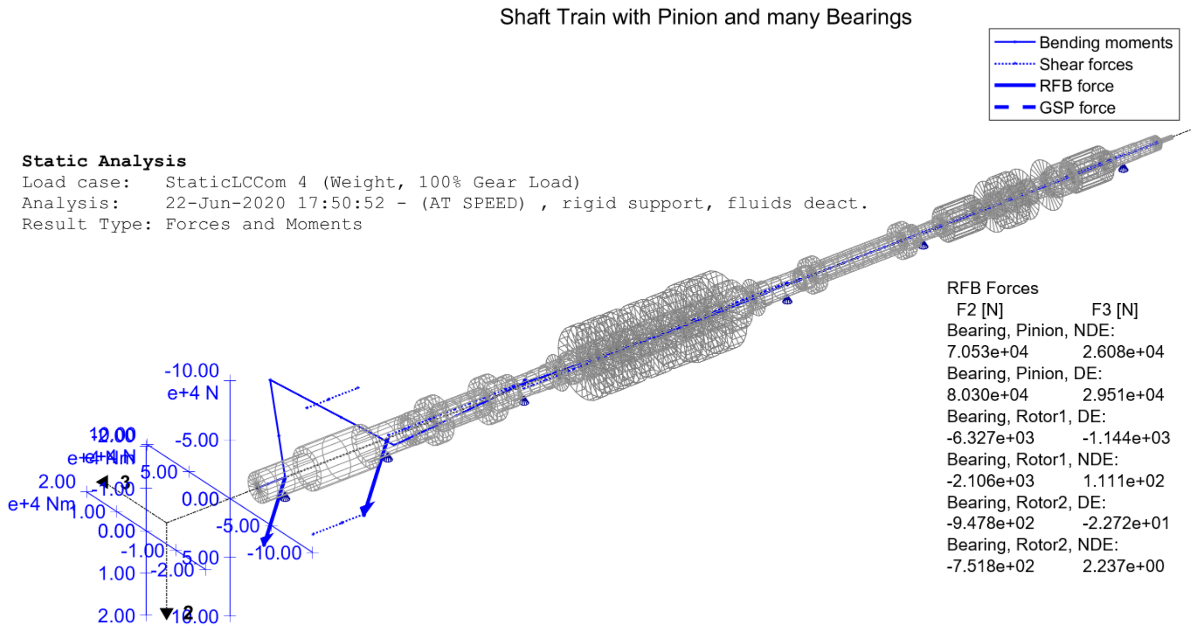

Fig. 1.5: Forces in the shaft train with many bearings, results with rigid bearings

1.2 Example of a Pump with many Seals

An example of a horizontal pump on two bearings with many seals is shown in figure 1.6. The seals are indicated with the green symbols. The bearings are 5-tilting pad bearings.

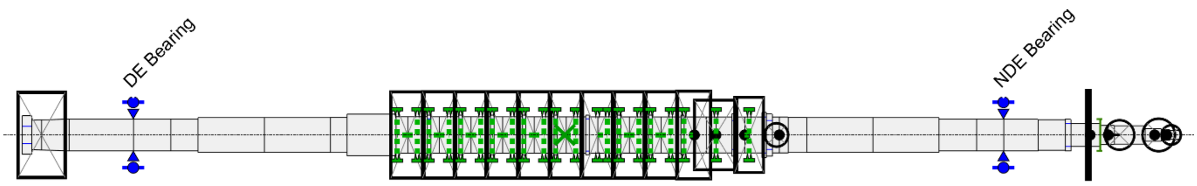

Fig. 1.6: Horizontal pump with seals

The static deformation and forces at 100% speed without fluids, i.e. in dry condition, are shown in figures 1.7 and 1.8. In figures 1.9 and 1.10 the same results are shown with fluids at 10% speed and in figures 1.11 and 1.12 at 100% speed.

Without fluids the displacements and bending moments are typical for a rotor under weight load. With the seal influence at 10% a horizontal component arises for the displacements and bearing forces caused by the cross-coupling stiffness of the seals. At 100% the seals have a big centring effect as can be seen in the displacements in fig. 1.11. The balance piston seal forces push the rotor practically into the centre. Since the seals, especially at the balance piston, contribute a lot to carrying the weight, the bearing forces are considerably smaller than at low speed as can be seen in figure 1.12.

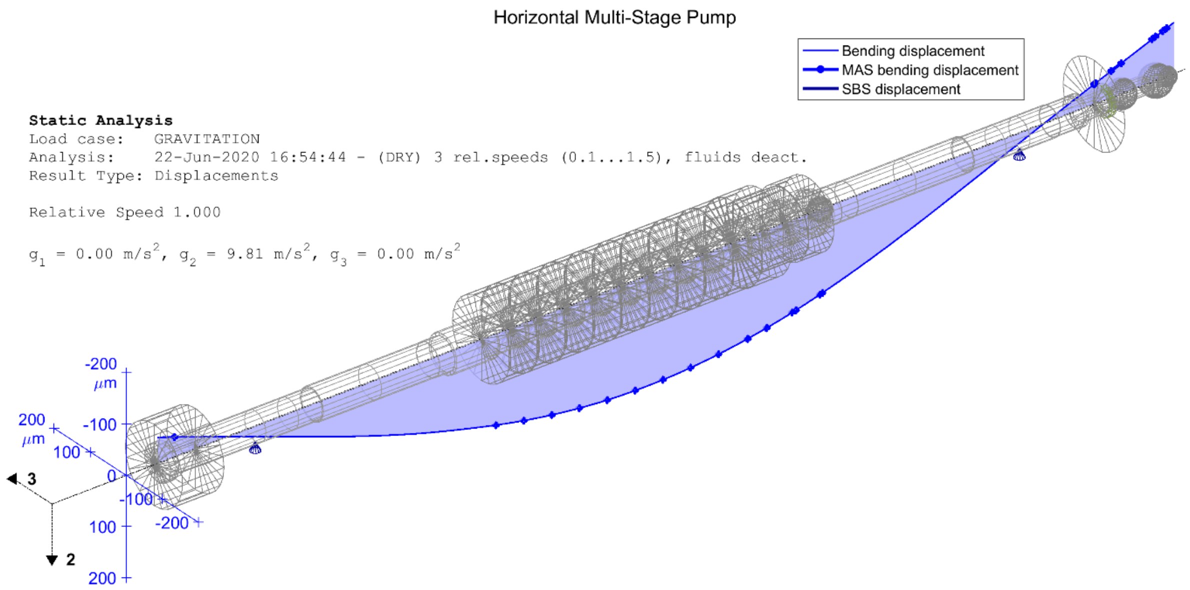

Fig. 1.7: Static displacements without fluids (dry), 100% speed

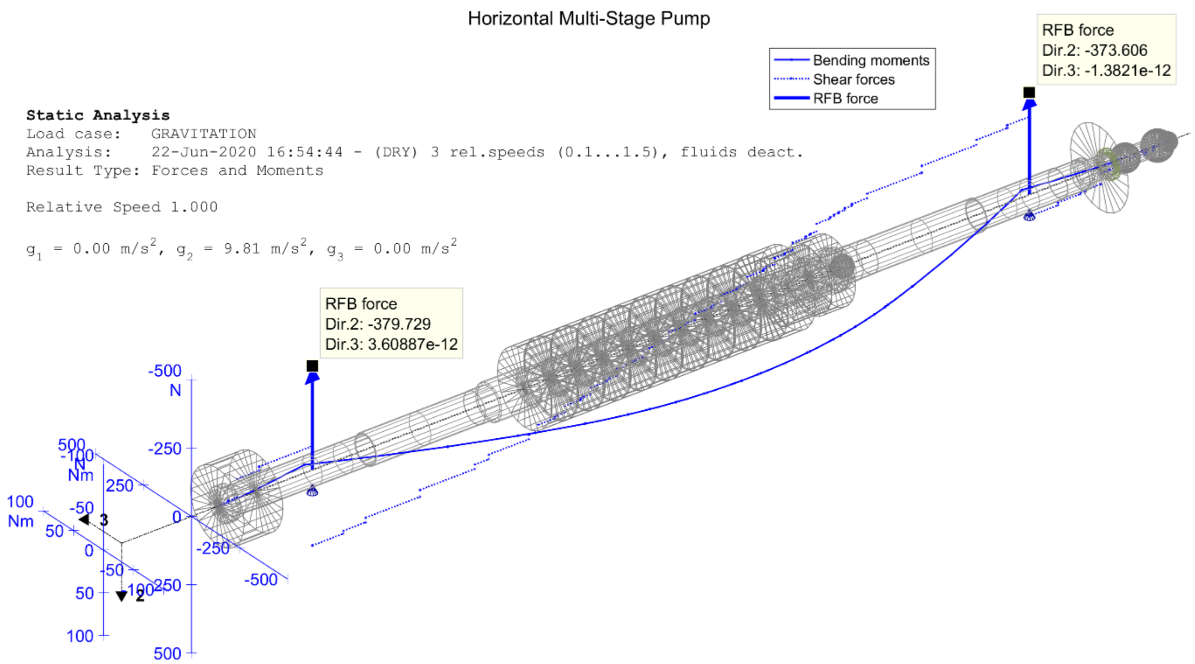

Fig. 1.8: Static forces without fluids (dry), 100% speed

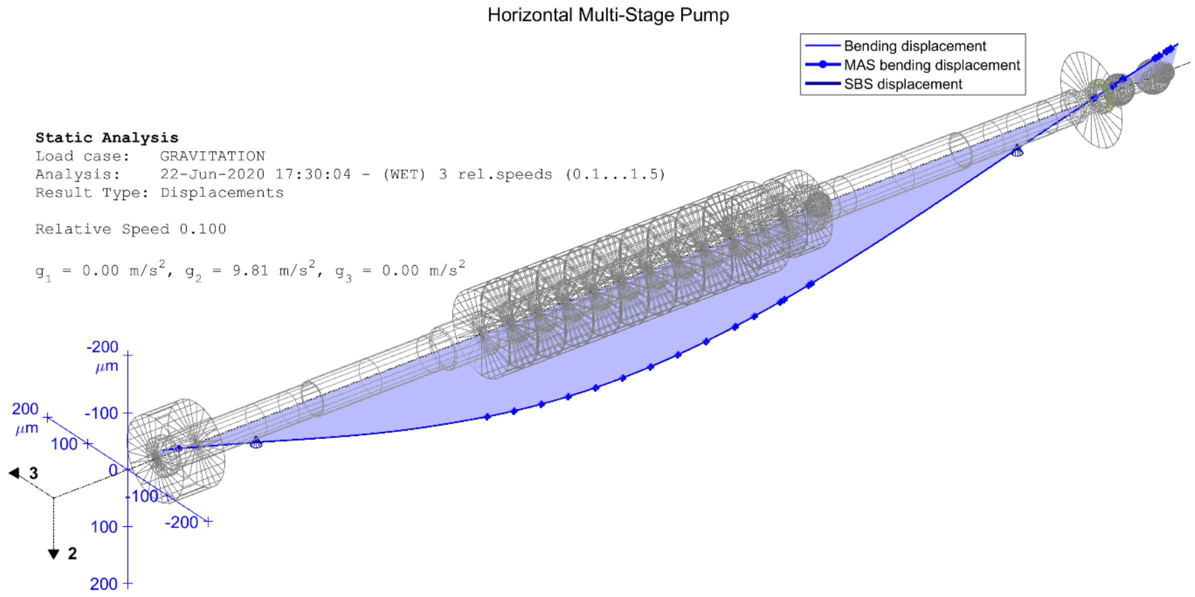

Fig. 1.9: Static displacements with fluids (wet), 10% speed

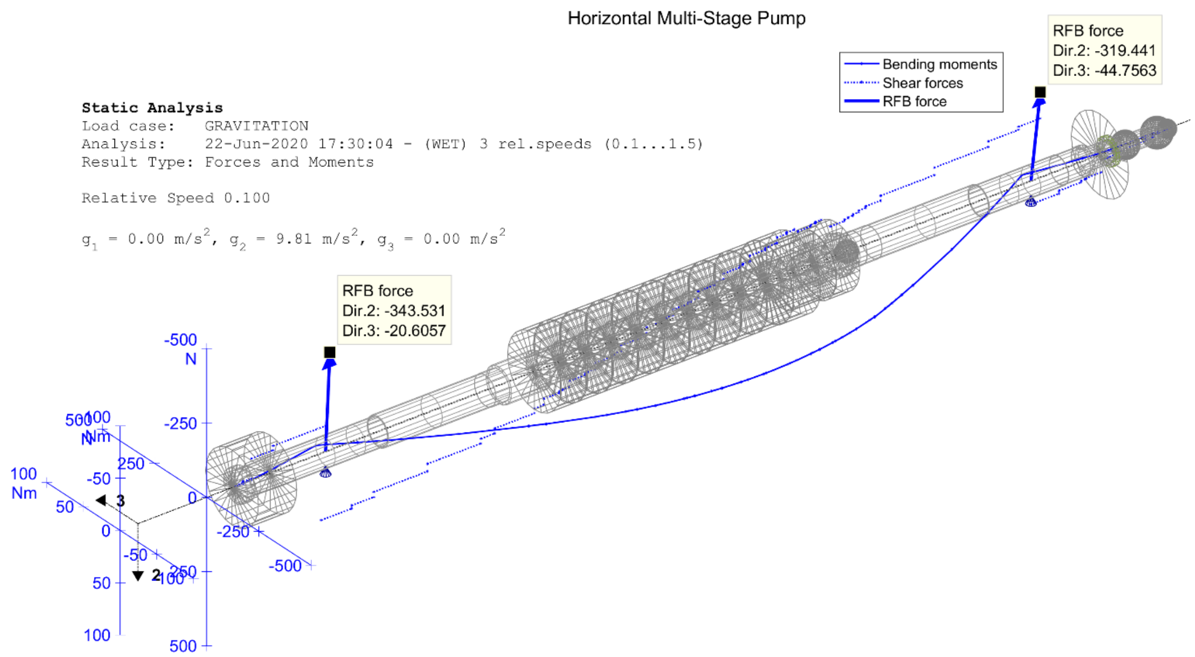

Fig. 1.10: Static forces with fluids (wet), 10% speed

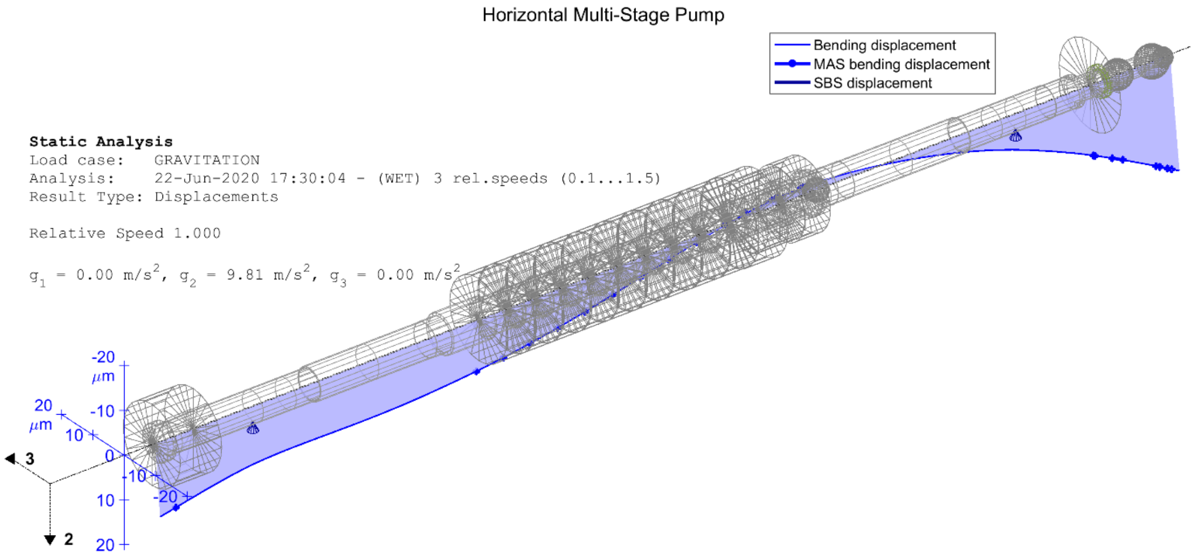

Fig. 1.11: Static displacements with fluids (wet), 100% speed

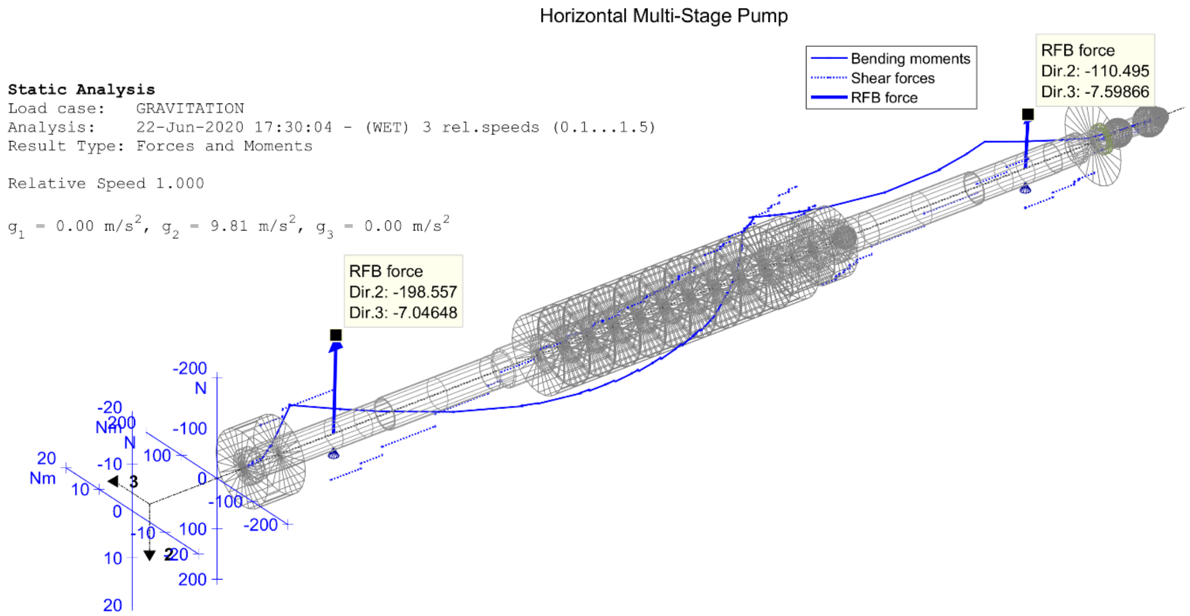

Fig. 1.12: Static displacements with fluids (wet), 100% speed

2. Automatic Analyses of Dynamic Fluid Bearing Characteristics

Since version 4.4 the coefficients of fluid film bearings in dynamic analyses such as Harmonic Response analyses, Campbell diagrams and other parameter variations no longer have to be pre-calculated in the Fluid Film Bearing object. In dynamic analyses speed ranges and static bearing loads are defined either by “Direct Load Input” or by the selection of a “Static Analysis Result”. When starting the analysis, the required coefficients are calculated automatically by creating adequate load case variants in the bearing object. In version 4.5 the load case variants have been improved. They are now created according to the rules described in table 2.1. Load case variants can also be extended if necessary.

It is obvious that the manual creation of load case variants can be cumbersome especially for examples as described in chapter 1 or in cases of speed dependent static bearing loads, especially with varying direction. For the RFB DIN analysis type the additional iteration for the actual mean temperature from a first table calculated with an estimated mean temperature adds to the problem of an adequate load variant. As can be seen in table 2.1 the speed range for each load is extended to ensure a sufficient So-range for the table of coefficients.

Table 2.1: Automatically created load variants in case of different loads and RFB analysis types

Bearing Analysis	Dynamic Analysis	Speed Steps N
Constant and variable adiabatic, So-similarity	With 1 speed, e.g. EIG or VSD	Speeds 80:10:120%, N=5
	With many speeds, e.g. CDG or HAR	Required speeds <=25, speeds as in analysis Required speeds > 25, $\Delta n=(n_{max}-n_{min})/(25-1)$, N=25
Variable adiabatic, no So-similarity	With 1 speed, e.g. EIG or VSD	Speeds 80:10:120%, N=5
	With many speeds, e.g. CDG or HAR	Required speeds <=50, speeds as in analysis Required speeds > 50, $\Delta n=(n_{max}-n_{min})/(50-1)$, N=50
DIN	With 1 speed, e.g. EIG or VSD	Speeds 64%,80:10:120%,144%, N=7
	With many speeds, e.g. CDG or HAR	Constant load: Required speeds <=25, speeds as in analysis + 80% n_{min} and 120% n_{max} Required speeds > 25, $\Delta n=(n_{max}-n_{min})/(25-1)$, $n_{min} : \Delta n : n_{max}$ + 80% n_{min} and 120% $n_{max,}$ N=25+2
		Speed dependent load F(n): Required speeds <=25, speeds as in analysis + 80% n_{min} and 120% n_{max} with extrapolated force + for each force 80% n and 120% n, N = 3 x analysis speeds + 2 Required speeds > 25, $\Delta n=(n_{max}-n_{min})/(25-1)$, $n_{min} : \Delta n : n_{max}$ + 80% n_{min} and 120% n_{max} with extrapolated force + for each force 80% n and 120% n, N=3x25+2

In the following automatically created load case variants for the static bearing loads are shown for the example of the gear compressor in figure 2.1. The loads are highly speed dependent due to the speed dependent driving and counter torques (see figure 2.2) causing speed dependent mesh forces. The system of the gear compressor is a lateral torsional coupled system.

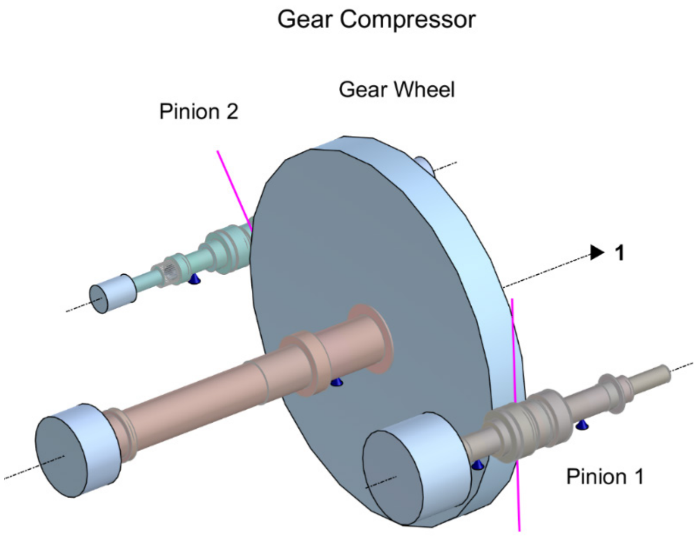

Fig. 2.1: Gear compressor

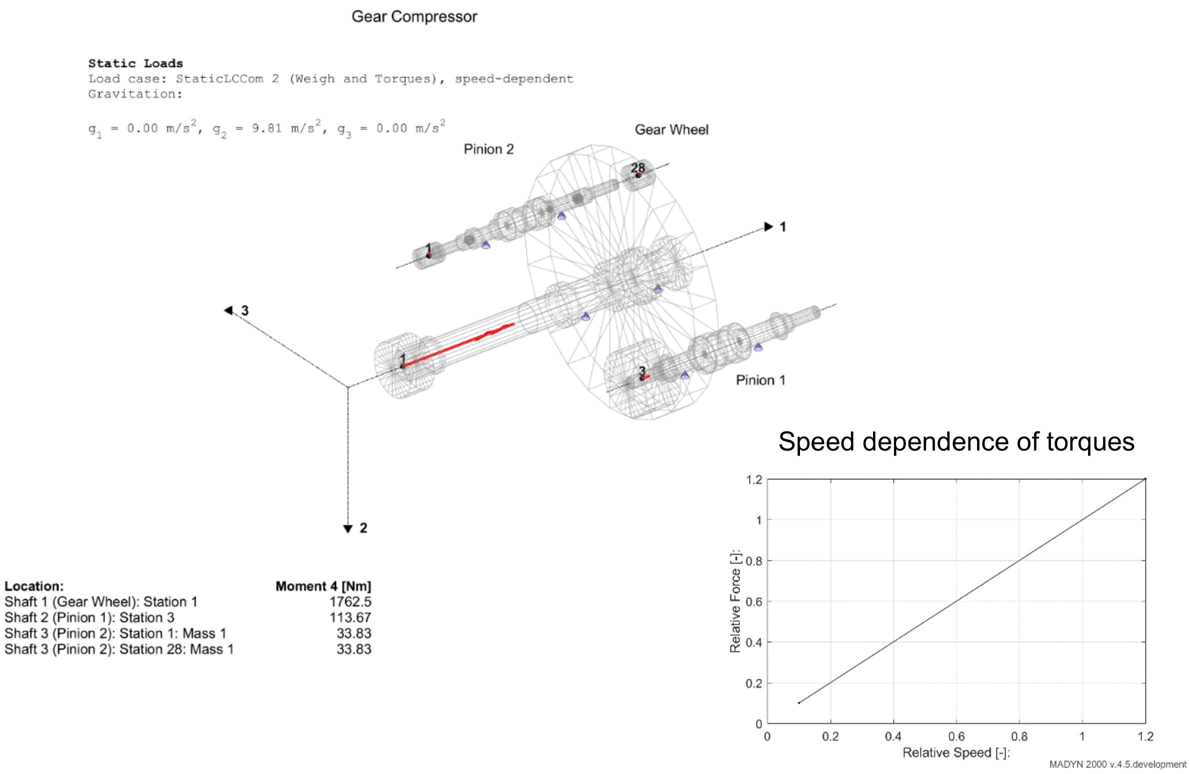

Fig. 2.2: Speed dependent driving torque and counter torques

The static deformations and forces due to weight and torques can be seen in figures 2.3 and 2.4. Since all rotors are statically determined and the main interest is the bearing loads, the analysis has been carried out with rigid bearings.

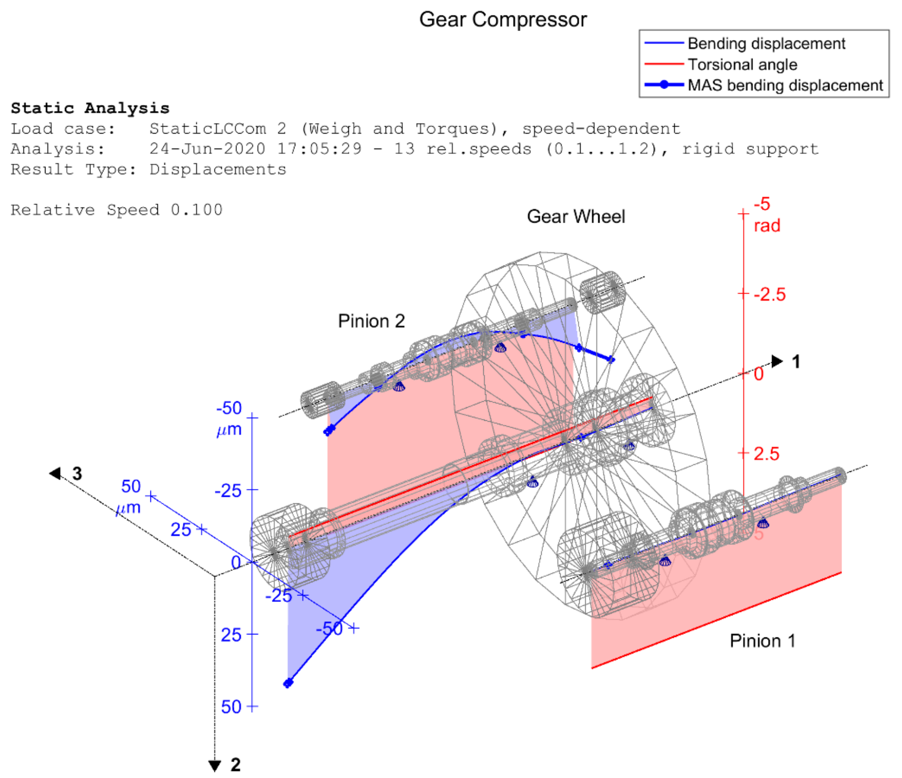

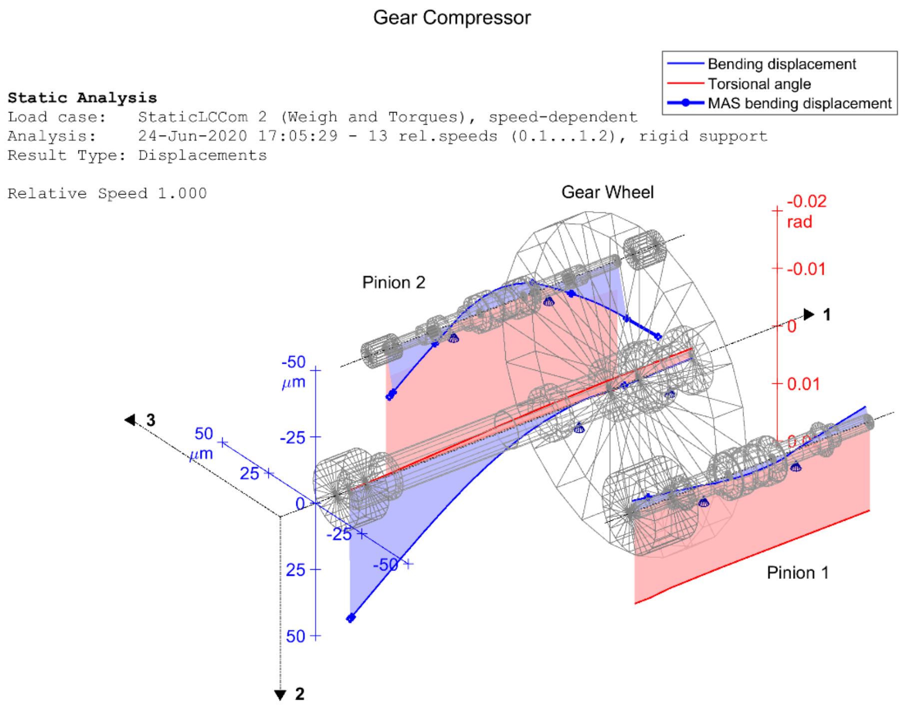

Fig. 2.3: Static deformation due to weight and torques at 10% and 100% speed

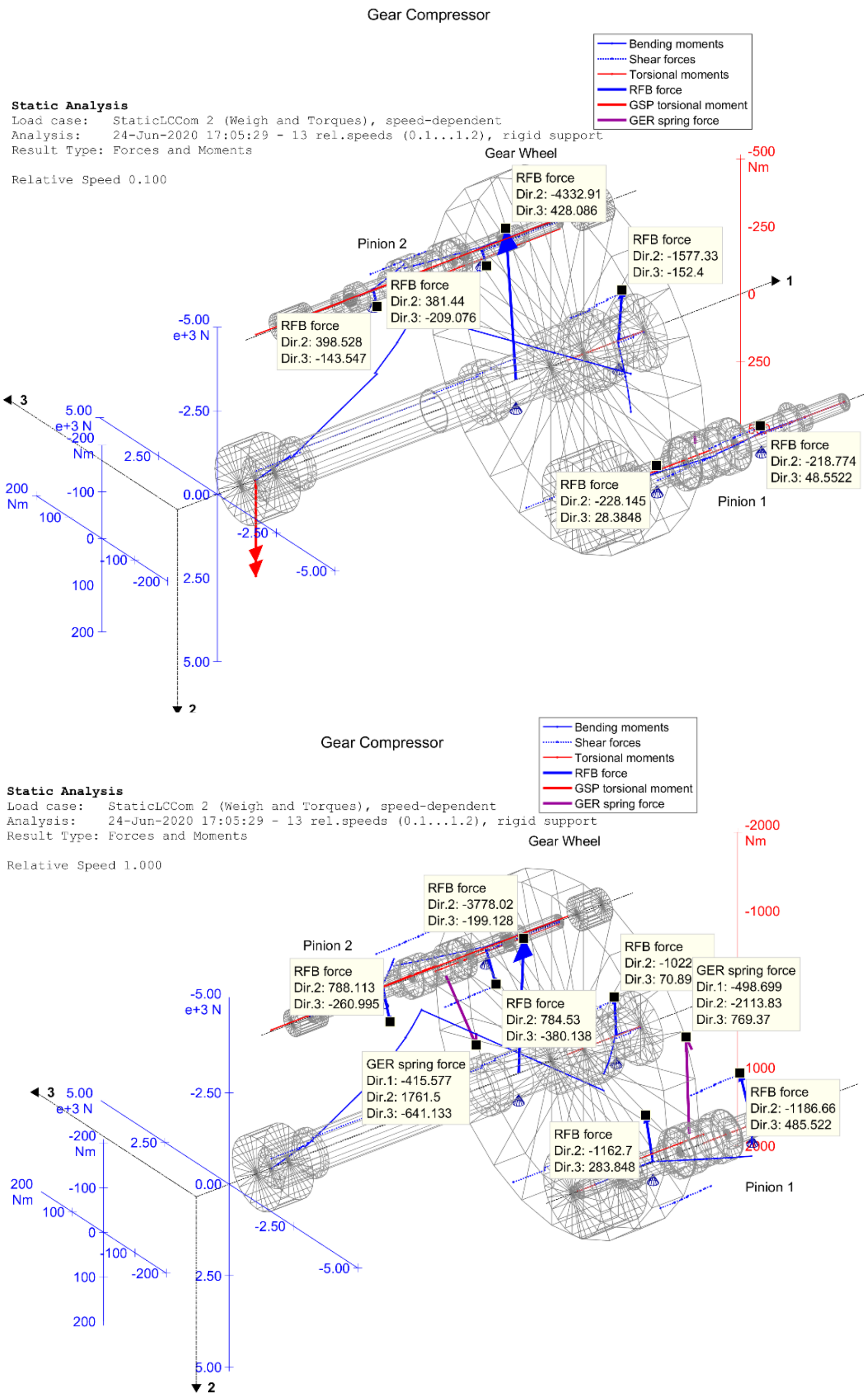

Fig. 2.4: Static forces due to weight and torques at 10% and 100% speed

It is obvious, that the static bearing forces vary a lot with the speed. They are quite different at 10% and 100% speed. For a better understanding of the bearing forces, the mesh forces (GER spring forces) are highlighted as well for 100% speed.

Calculating a Campbell diagram with a speed range from 15% to 120% speed with 15 different speeds automatically creates load case variants in the RFB objects and starts the ALP3T analysis for the rotordynamic bearing coefficients. The static results of the ALP3T analysis with the load, the So-numbers and the shaft centreline curve in the bearing (Gümbel-curve) for all bearings are shown in the figures 2.5 to 2.7. The load variants are created according to the rules in table 2.1. In case of less than 50 required speeds and analysis type “variable adiabatic” the same speeds as in the Campbell diagram are used. The resulting Campbell diagram is shown in figure 2.9. It is rather complex for such a lateral torsional coupled system of a gear with a wheel and two pinions.

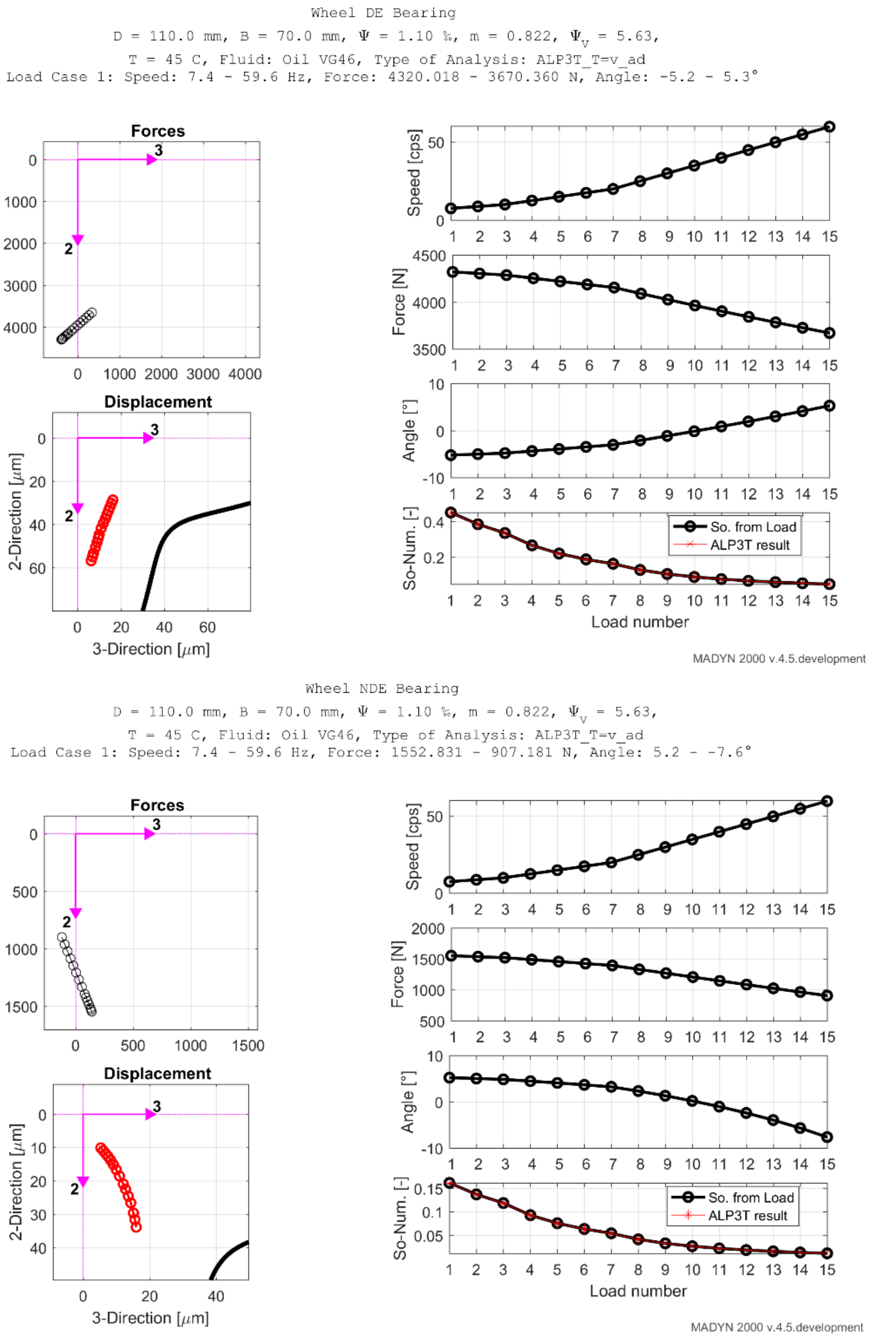

Fig. 2.5: Load case variants created for the wheel bearings in the Campbell diagram analysis

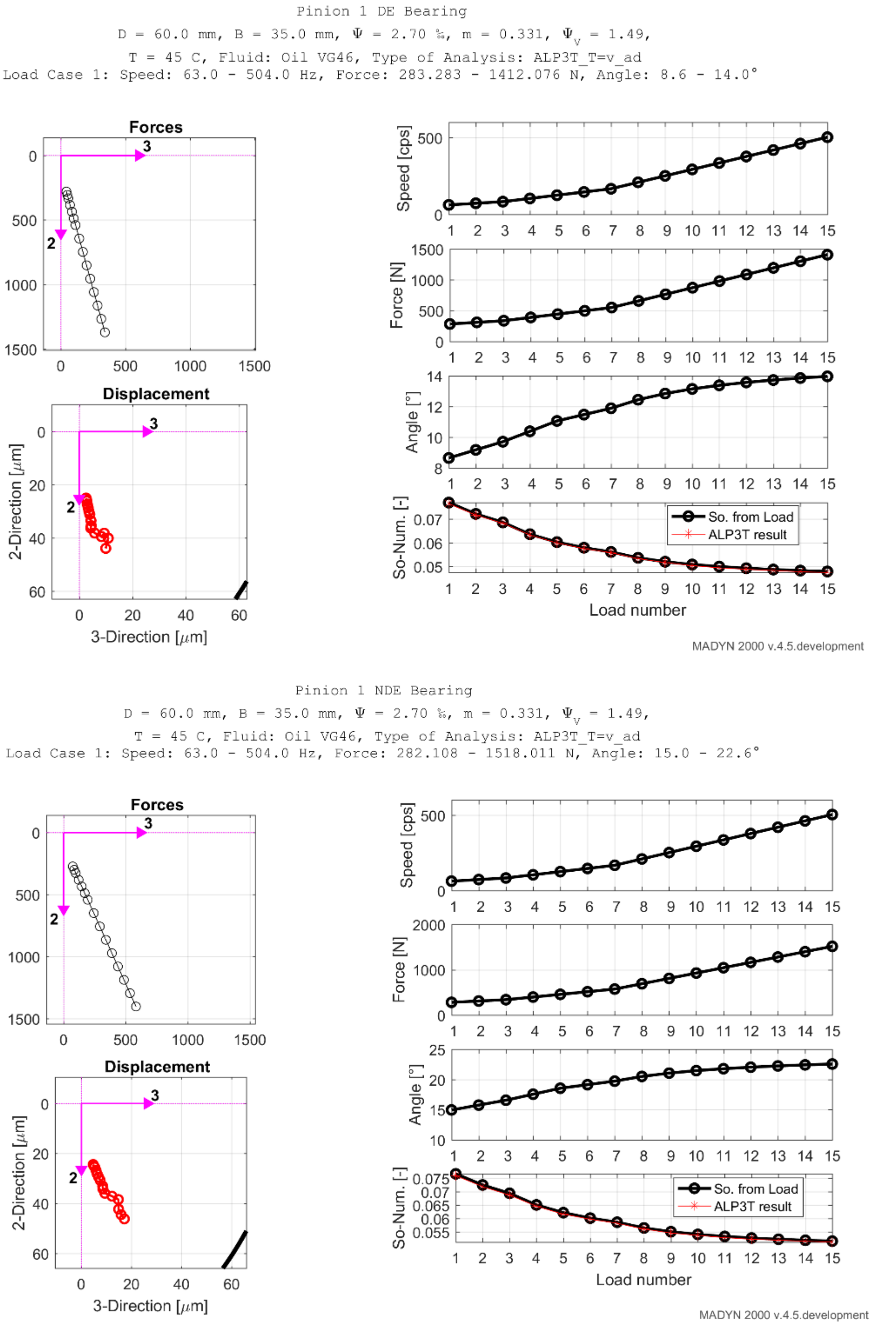

Fig. 2.6: Load case variants created for the pinion 1 bearings in the Campbell diagram analysis

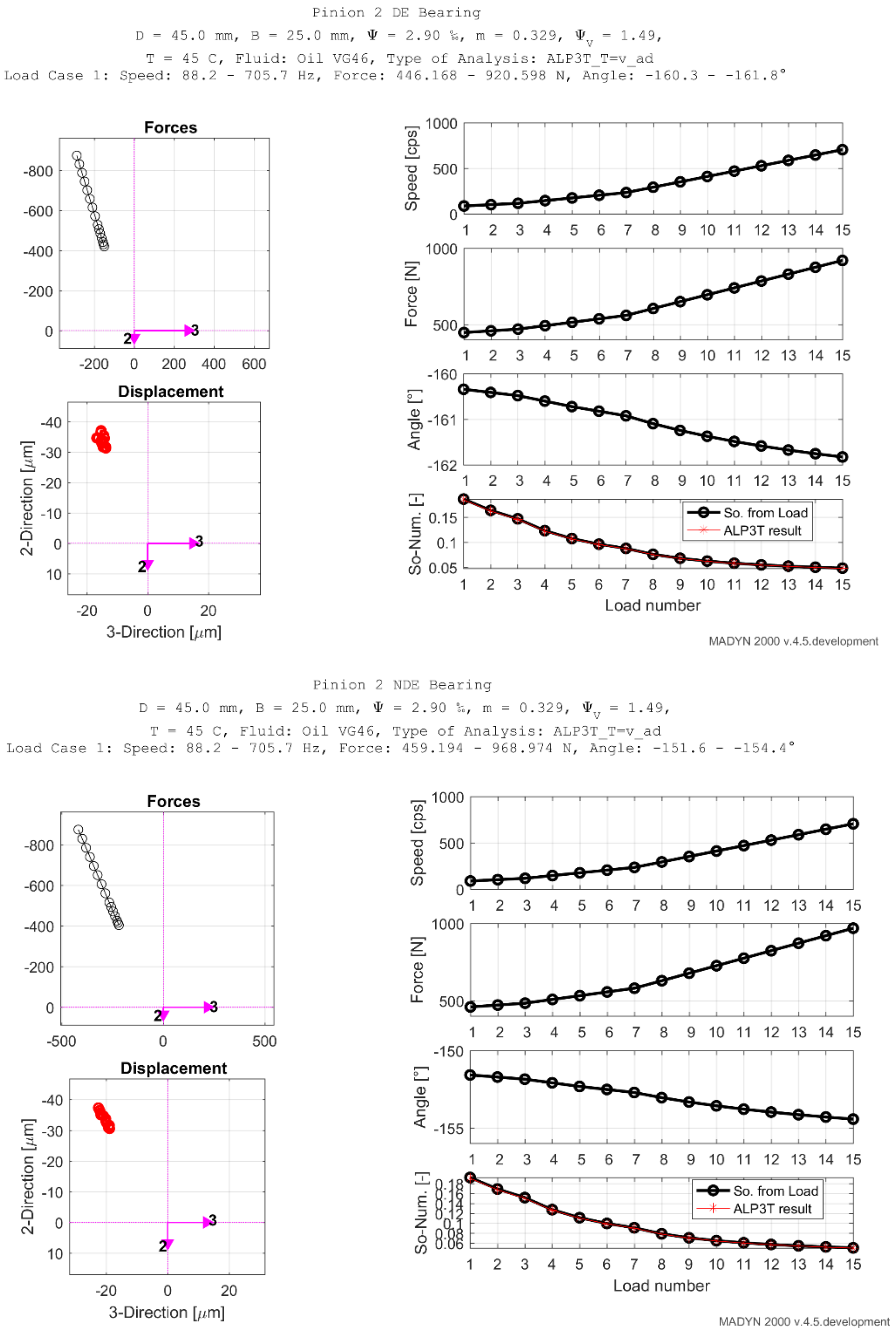

Fig. 2.7: Load case variants created for the pinion 2 bearings in the Campbell diagram analysis

In case the analysis type of the bearing is not "variable adiabatic" but DIN the automatically created load case variants are different (see table 2.1). For a speed dependent static force F(n) additional speeds 80% and 120% for each force are calculated. Moreover, the forces at the lowest and highest speed are extrapolated to 80% minimum speed and 120% maximum speed and analysed. This yields 3x15+2=47 loads. They are shown in figure 2.8 for the wheel bearing of the gear compressor.

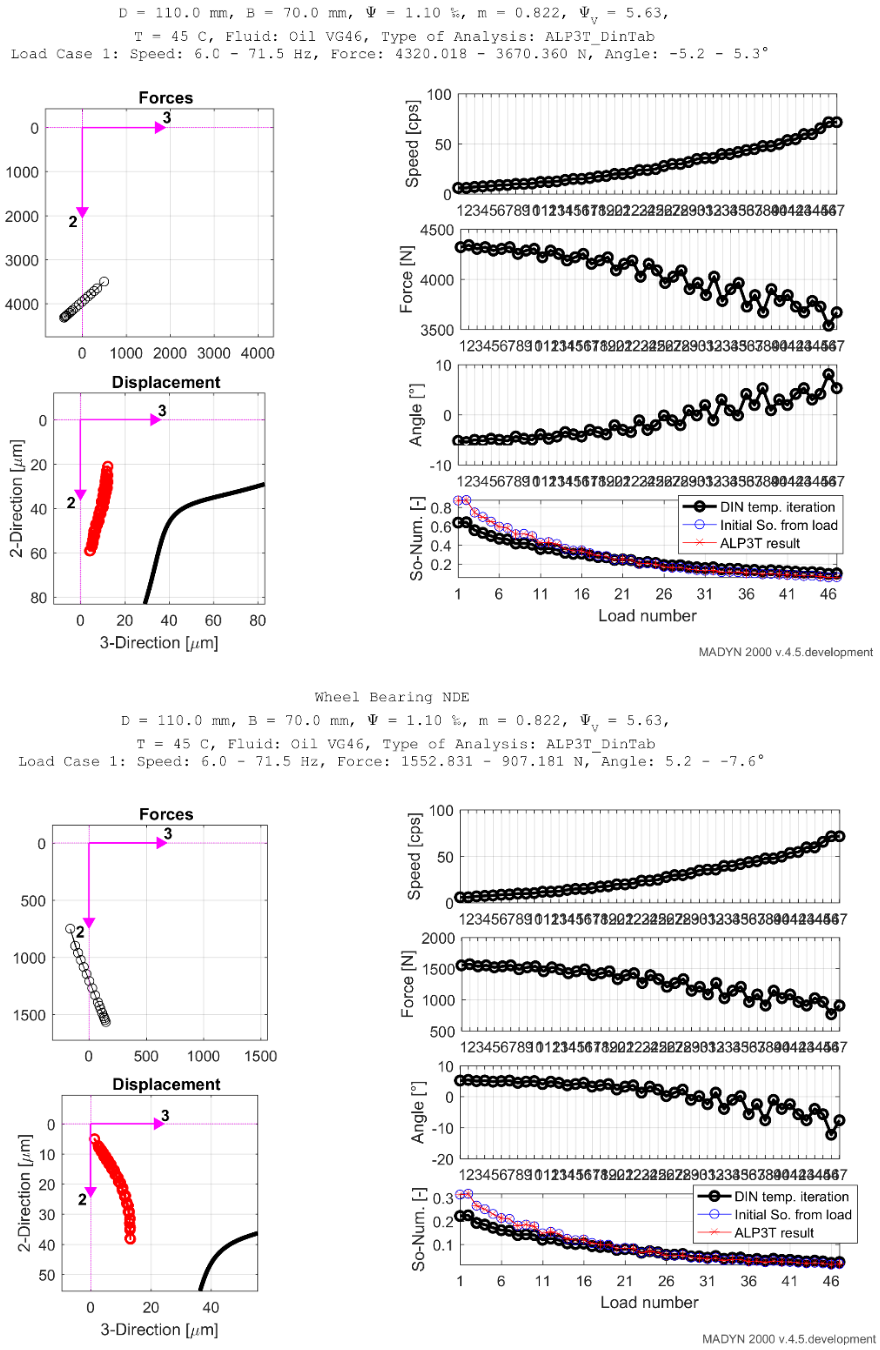

Fig. 2.8: Load case variants DIN analysis created for the wheel bearings for the Campbell diagram

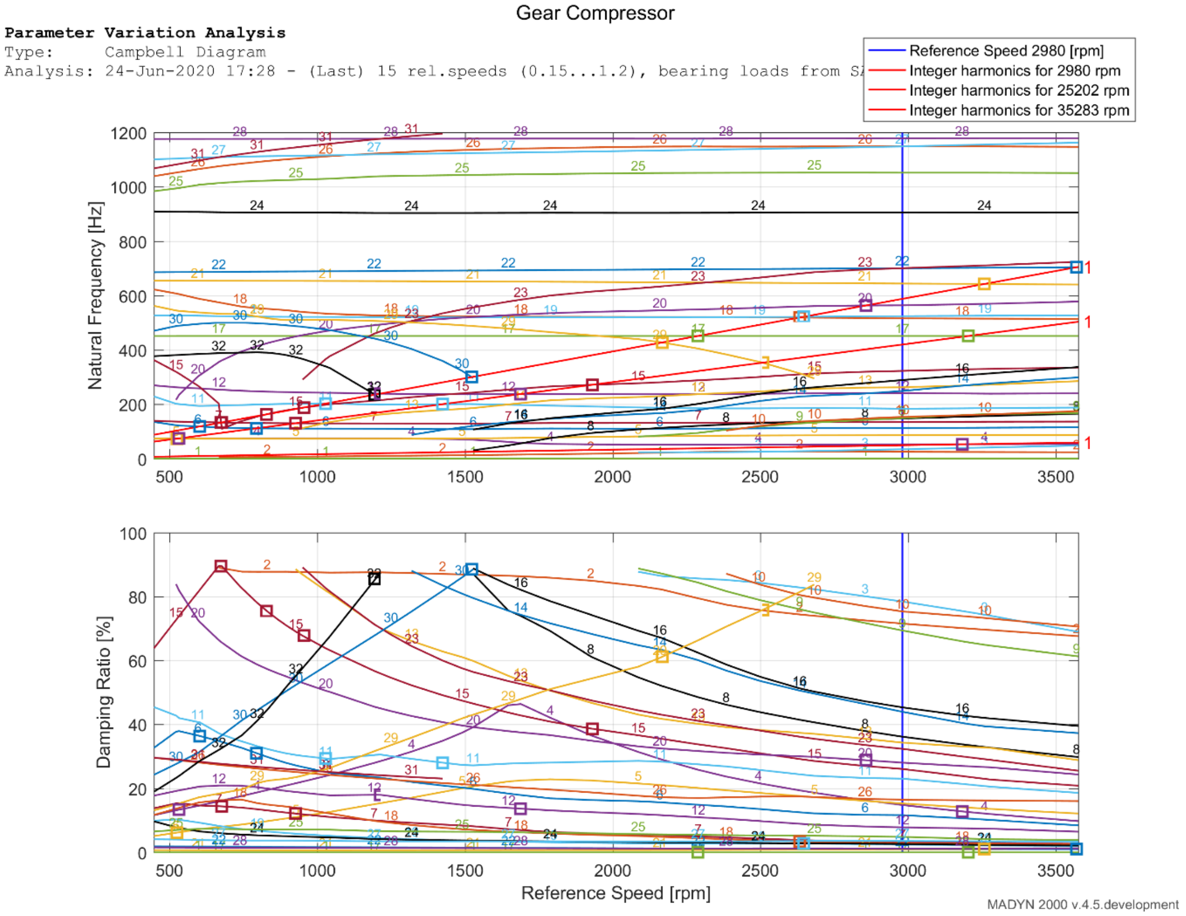

Fig. 2.9: Campbell diagram of the lateral torsional coupled system of a gear compressor

3. New Features for User Defined Fluids (FDC)

User defined fluids allowing the analysis of the rotordynamic coefficients from geometry, fluid and operating data with a specialized CFD program have been introduced in version 4.4. In this program the flow in the seal is calculated. In a first step the centred position is analysed in a 2D analysis. In a further step a 3D perturbation analysis of the centred solution is carried out to calculate rotordynamic coefficients. For the perturbation, the rotor is moving on an orbit with different precession frequencies. For more details see the documentation of MADYN 2000.

In version 4.5 some more features for user defined seals are introduced, as described below.

3.1 Geometry and Grid Plots

The geometry of a seal together with the grid can be plotted now. A new item was added to the plot menu for this purpose (see figure 3.1). An example for the geometry plot is shown in figure 3.2.

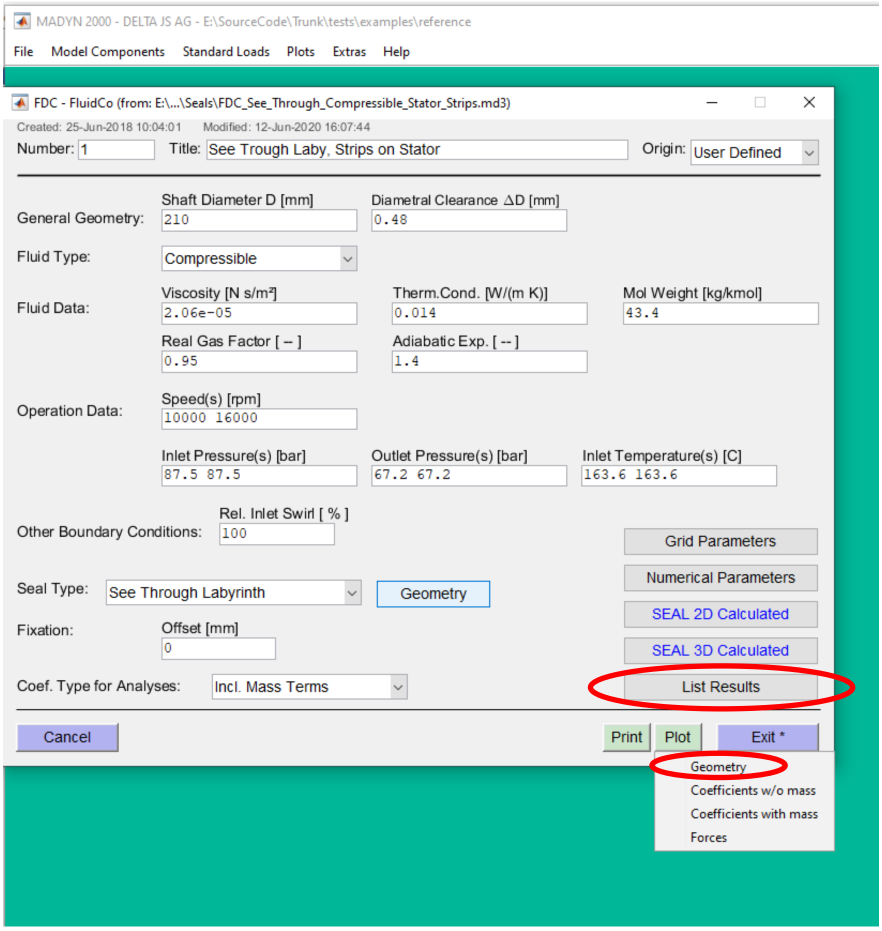

Fig. 3.1: GUI for user defined FDC with additional item for the geometry

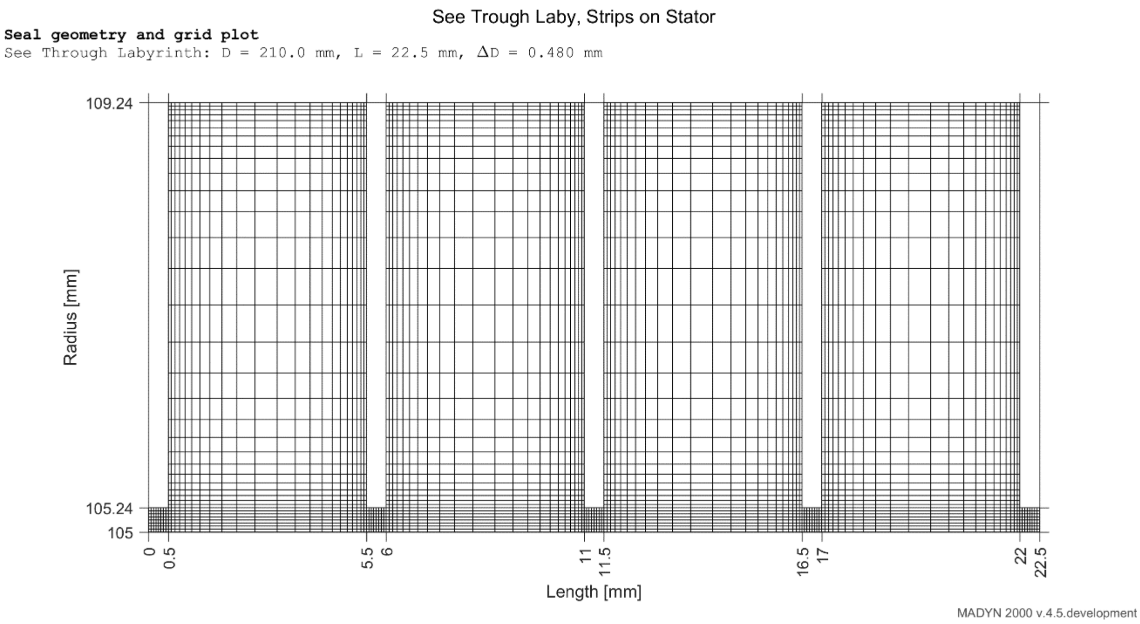

Fig. 3.2: Seal geometry plot

3.2 Field Plots of Results

Field plots of the results of the 2D analysis are available now. The following 2D fields can be plotted:

- Pressure
- Temperature
- Fluid density
- Velocities in axial, radial and circumferential direction
- Turbulence energy k (see explanations to k-ε model in /1/)
- Turbulence dissipation ε (see explanations to k-ε model in /1/)
- Apparent viscosity, sum of laminar and turbulent viscosity resulting from k, ε (see /1/)

The field plots are called as follows from the FDC GUI for user defined seals: The button “List Results” (see figure 3.1) opens the window shown in figure 3.3. In the window the operating parameters and seal coefficient are shown. The coefficients are only shown if the 3D analysis has also been carried out. The button “2D Result Plots” is activated, if one or several results in the list are selected (highlighted in grey). It opens the GUI in figure 3.4 to select field plots by check boxes. In figure 3.5 a plot with the probably most important results (pressures and velocities) is shown for the seal in figure 3.2 with the operating parameters highlighted in figure 3.3.

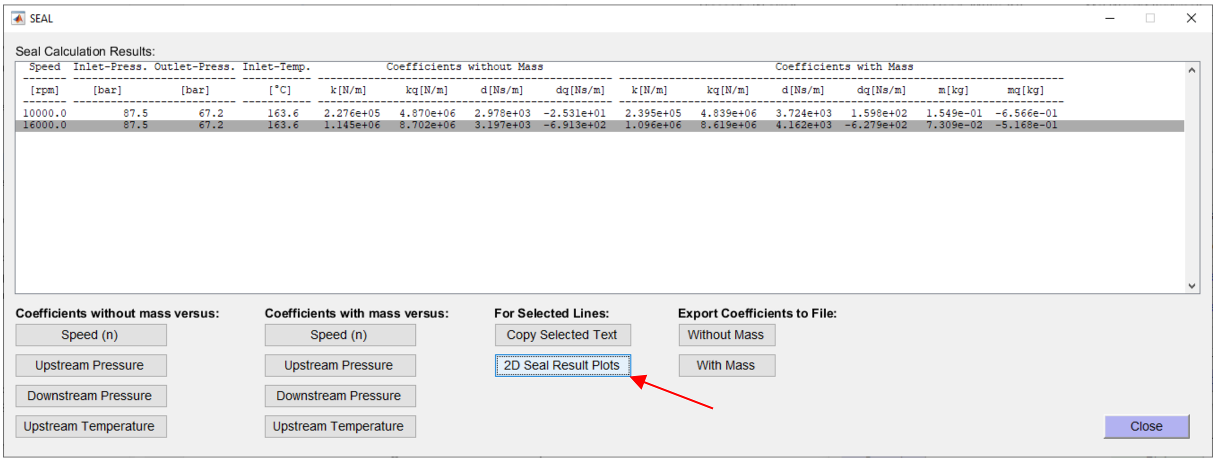

Fig. 3.3: GUI to call field plots

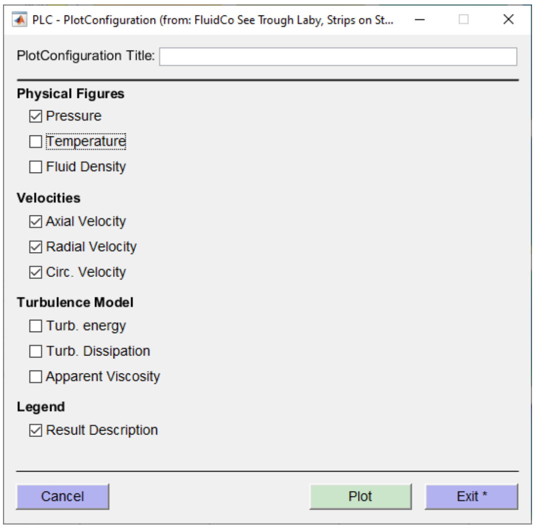

Fig. 3.4: GUI to select field results for 2D plots

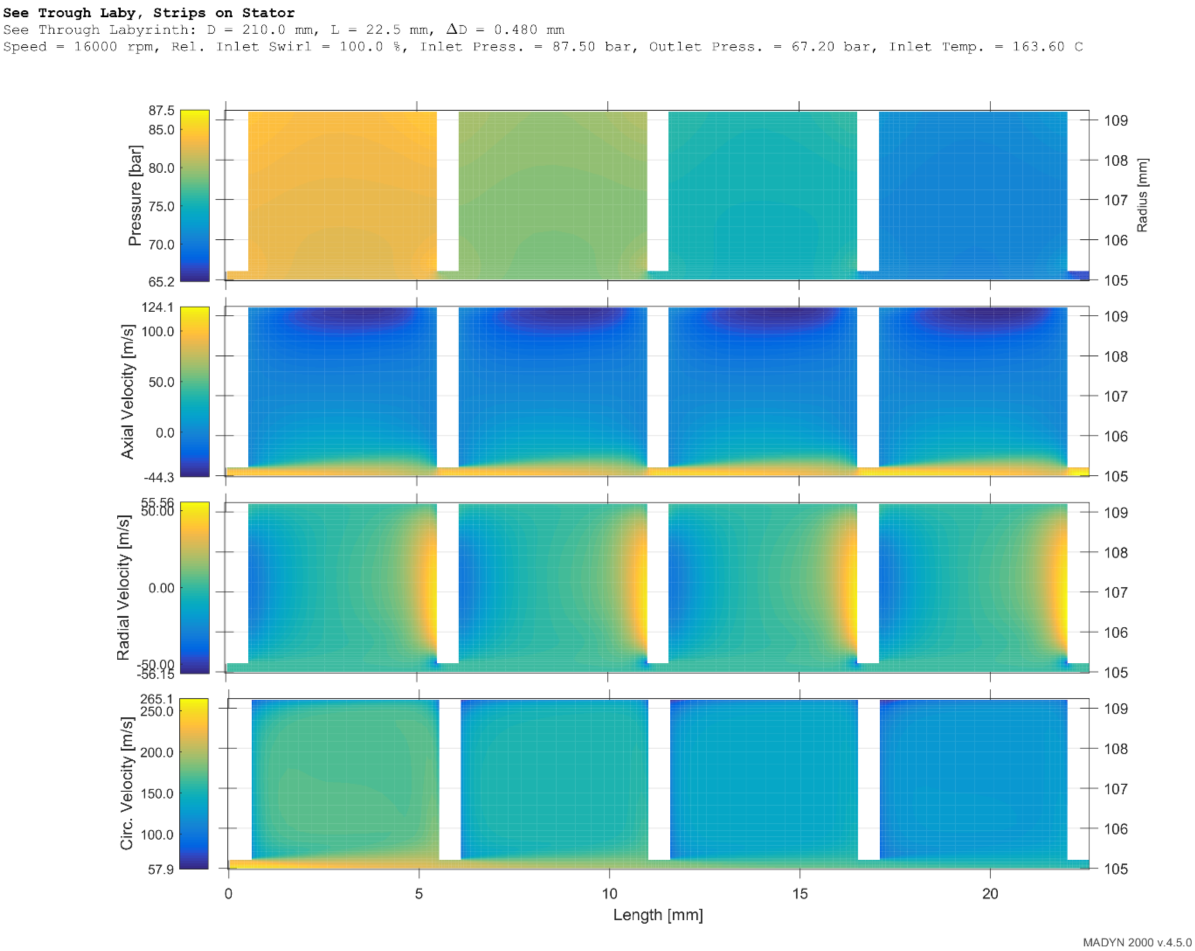

Fig. 3.5: Field plots of 2D results

4. Improvements of Connections

In MADYN 2000 various connections are available. Some connections and some special objects can cause so called master / slave relations. In table 4.1 examples of such relations are shown.

Table 4.1: Examples of connections and objects with master / slave relation

Object, Connection	Master	Slave
Mass (MAS) with offset	Shaft station, where MAS is fixed.	Node with distance to fixation
Fluid (FDC) with offset	Shaft station, where FDC is fixed.	Node with distance to fixation
Rigid connection of shafts	Shaft station	Shaft station
GSP connection with inf	Shaft station	Shaft station
SBS connection (shaft in shaft)	SBS node	Outer shaft station

In case of the objects with offset an additional node is introduced. In case of MAS it is the centre of gravity, which is not necessarily be at the same location as the fixation. In case of FDC it could be the centre location of an impeller shroud seal, which may have a distance to the impeller fixation on the shaft. The distance between the station of fixation and the additional node is bridged with a rigid element causing a master / slave relation.

In the rigid shaft connections and GSP connections with stiffness inf[1] for one or several coordinates one of the connected shaft stations is a slave to the other station, they cannot move independently.

The existence of slave nodes can cause problems in some configurations. Moreover, slave master relations cannot be generally combined. In table 4.2 such cases are shown. The problematic cases could not be processed in version 4.4 without workarounds such as attaching objects to nearby stations. The user was informed in such cases with a message. In version 4.5 most of these cases can be handled, thanks to a sophisticated switching mechanism (attaching object to master instead of slave). There are still a few exceptions, where switching is not possible, as explained below.

Table 4.2: Problematic cases caused by slaves

	Case	Problem	Handling in version 4.5
1	Radial bearings, general springs and speed dependent fluids attached to outer shaft station of an *SBS connection*.	Outer shaft node is a slave → rotordynamic coefficients cannot be added to a slave, rotordynamic coefficients cannot be varied in parameter variations VSD, slaves cannot be used as input to or output from active systems.	Objects are added to SBS master node.
2	MAS or FDC with offset attached to outer shaft station of an *SBS connection*.	Outer shaft node is a slave → Master of master / slave relation cannot be added to slave.	MAS or FDC are added to SBS master node.
3	Objects attached to *rigid connection*.	Station could be slave → Similar problems as in case 1 and 2	Objects are always attached to master.
4	Objects attached to station with *GSP connection with inf* for some coordinates.	Station could be slave → Similar problems as in case 1 and 2	Check if object can be moved to master. Yes, object is moved. No, check if master and slave can be switched. Yes, switching of stations No, error message.

The situation of case 2 with an FDC with offset is shown in figure 4.1.

For case 4 the situation that an object cannot be moved occurs for example in case of a lateral system with a MAS with offset attached to one shaft at the same station as a GSP connection with inf for the radial displacements (2,3 directions) to another shaft. Moving the object to the other shaft would have the same effect for the lateral inertia, however not for the moments of inertia of the MAS object about the 2 and 3 directions (5,6 directions). Therefore, moving is not possible. In such a case master and slave of the GSP connection are switched. In general, this will be possible, however, if

[1] Stiffness inf (infinite) means rigid.

the new slave has an object attached such as a bearing this solution is not viable. An error message will then appear with a suggestion for a workaround, such as replacing inf with a high stiffness.

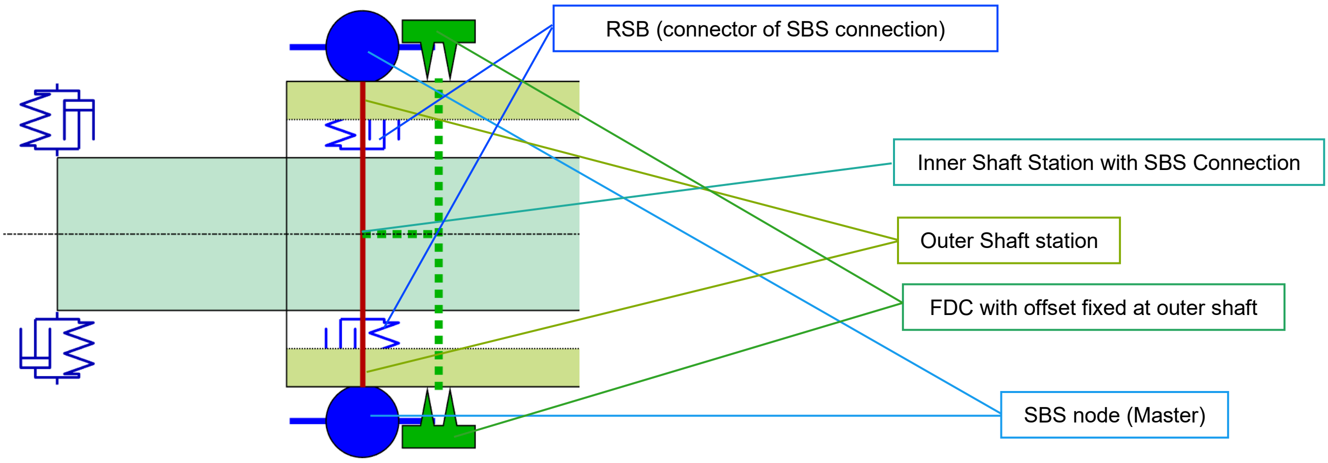

Fig.4.1: SBS connection, MAS with offset attached to outer station

In case of static analyses (SAN) with rigid bearings with SBS connection the inner shaft node also becomes a slave due to the rigid connection to the SBS master. In this case no MAS with offset or FDC with offset must be applied at the inner shaft of the connection. An error message will appear when trying to run a SAN rigid analysis with such a system.

In the following a case is shown, allowing easier modelling thanks to improvements of connections. It is a rolling element bearing combined with a squeeze film damper with a centring cage at the outer ring. Such supports are frequently used in aeroengines. The system in figure 4.2 is a compressor of an aeroengine. The models of the downstream shaft end with the squeeze film dampers are shown in figure 4.3. The stiffness of the centring cage is modelled as a GSP. A further GSP is used as axial support at the right end of the ring. On the left side the old model with 3 sections of the squeeze film damper ring is shown, whereas on the right side the new model with only 2 sections is shown. The 3 sections were necessary, because the outer squeeze film damper could not be at the same station as the SBS connection with the rolling element bearing used as connector, because the station of the outer shaft is a slave of the SBS node. In version 4.5 this is no longer a problem, they can be at the same station.

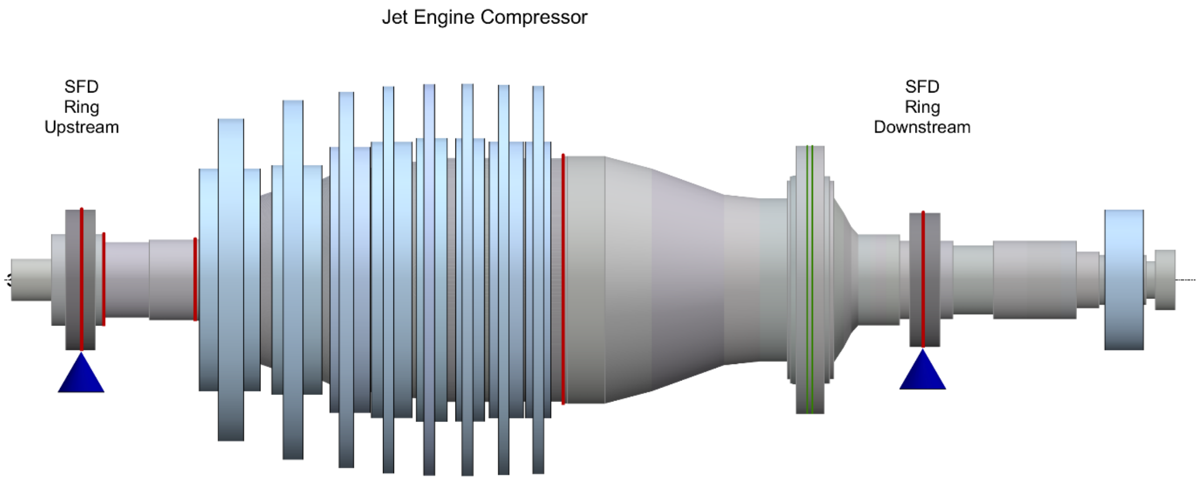

Fig. 4.2: Jet engine compressor

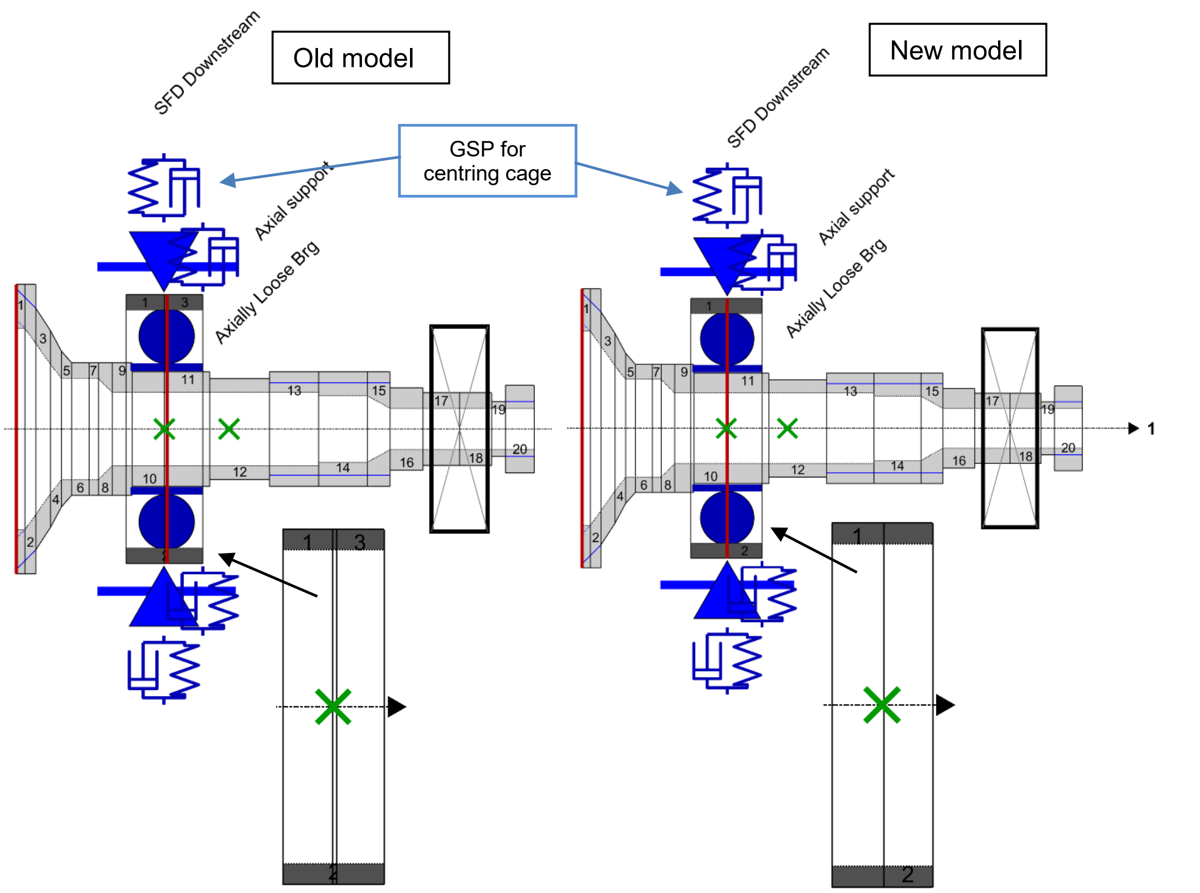

Fig. 4.3: Downstream shaft end with rolling element bearing and squeeze film damper

5. Improvements of Fluid Film Bearing Analyses

5.1 Pocket Reverse Flow

In version 4.5 a pocket reverse flow is considered. It can occur between two pads, if the flow at the exit of one pad is too large to enter the gap of the next pad. In this case the pressure in the pocket can get higher than the pocket pressure (negative pressure difference) causing a reverse flow of hot oil. In case of a sealed bearing it will re-enter the bearing at other pockets. This may lead to slightly higher temperatures in the bearing than in previous versions. The effect plays a role at higher bearing loads.

The consequences of this effect are shown for the tilting pad bearing in figure 5.1. Further data of the bearing are:

Speed:	10’000rpm
Fluid:	Oil VG46
Inlet temperature:	48 °C
Bearing load:	72’000 N → specific pressure: 20 bar
Nozzle area (direct lubrication):	34.5 mm^2
Inlet pressure in front of nozzles:	1.8 bar gauge

The analysis is a variable adiabatic analysis with 2-phase flow.

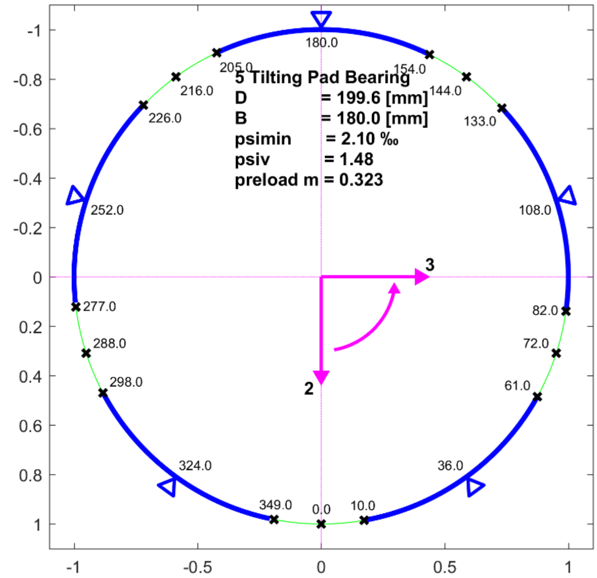

Fig. 5.1: 5-Tilting pad bearing as example to show reverse flow effect

2D plots of the minimum oil film thickness as well as the maximum, mean and pad temperatures are shown in figure 5.2. The lower 2 pads 1 and 5 have the smallest oil film thickness, the upper pad 3 the largest clearance. Transitions of the flow from larger clearance to smaller clearance are between pad 3 to 4 and to a higher extent from 4 to 5. Between pad 4 and 5 there is no temperature drop due to fresh oil for this reason. Most clearly this can be seen in the mean temperature plot.

For comparison, the same results calculated with version 4.4 are shown in figure 5.3. Temperatures between pads are about 4°C lower and the maximum temperature is about 2°C lower.

The effect of this difference on the rotordynamic coefficients are minimal, as can be seen in figure 5.4.

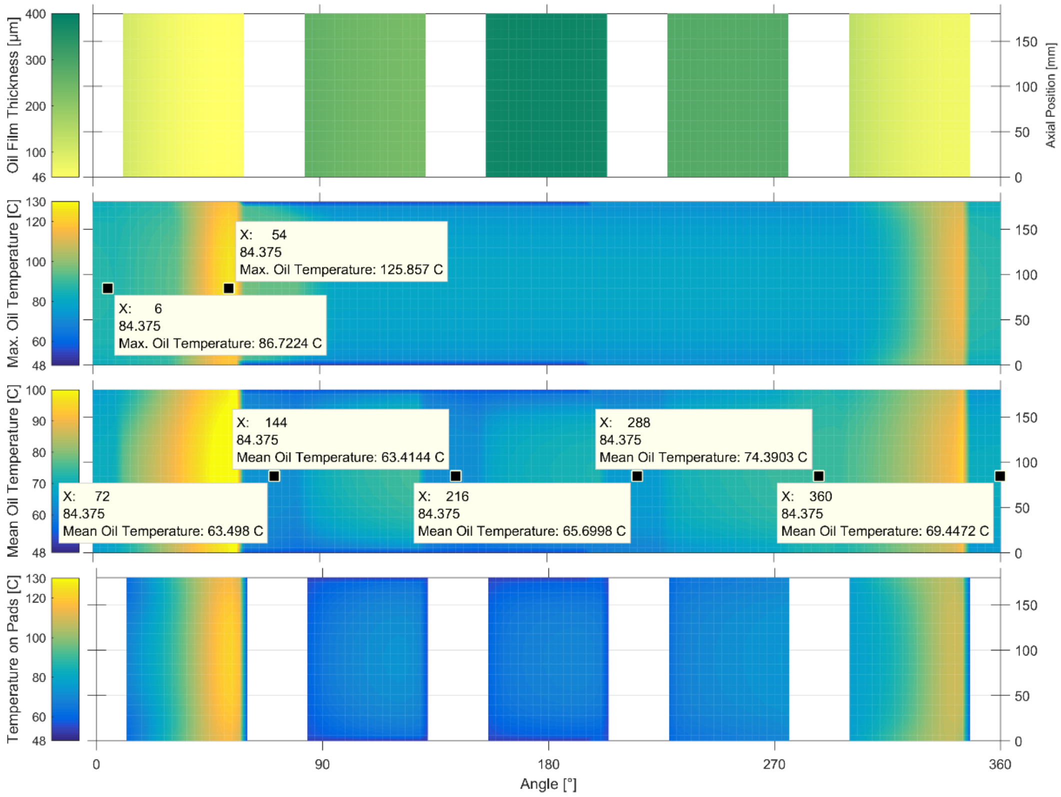

Fig.5.2: Minimum oil film thickness and temperatures

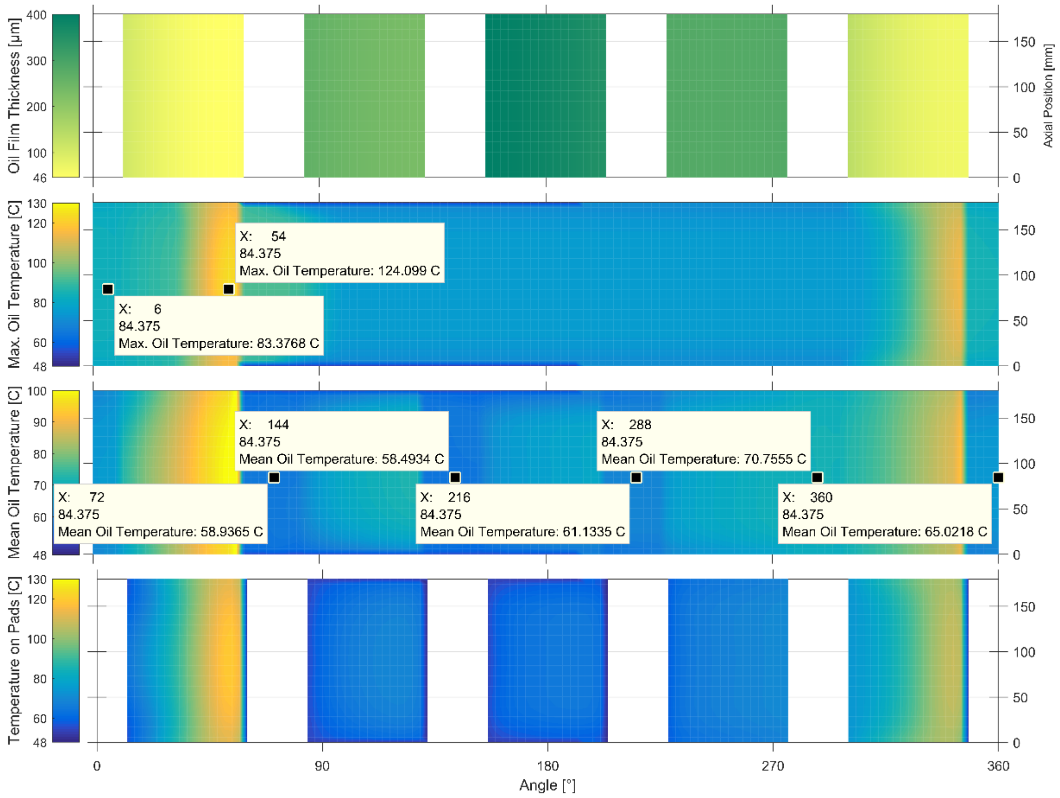

Fig.5.3: Minimum oil film thickness and temperatures calculated with version 4.4

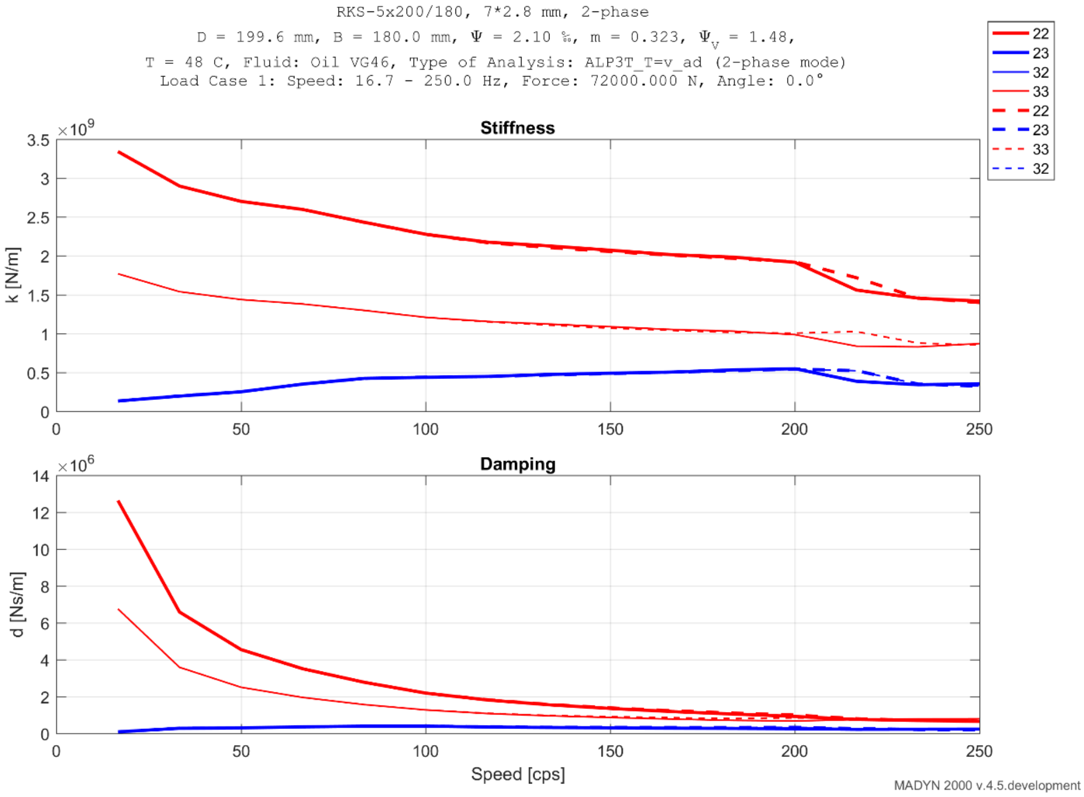

Fig. 5.4 Rotordynamic coefficients calculated in versions 4.5 and 4.4 (dashed lines)

5.2 Other improvements

Further improvements for bearing analyses were introduced in version 4.5 increasing the robustness and speed of analyses.

6. References

/1/ H.P. Weiser: Ein Beitrag zur Berechnung der dynamischen Koeffizienten von Labyrinthdichtungssystemen bei turbulenter Durchströmung mit kompressiblen Medien. Dissertation TU Kaiserslautern 1989.